COSMIC RAYS INTERFACING ASTROPHYSICS AND PARTICLE PHYSICS*

Heinigerd Rebel

Forschungszentrum Karlsruhe — KASCADE collaboration
P.O.Box 3640, D-76021 Karlsruhe, Germany
e-mail: rebel@ik3.fzk.de

(Received April 11, 2000)

The development of Extensive Air Showers (EAS) is driven by the hadronic interactions of the primary and secondary particles with the atmospheric nuclei. Hence a careful analysis of the EAS appearance, in particular of the hadronic component, provides valuable information on features of the hadronic interaction. Especially, in ultrahigh energy regions extending the energy limits of man-made accelerators and the experimental knowledge from collider experiments, the hadronic interaction is subject of uncertainties and debates. Since the EAS development is dominantly governed by soft processes, which are not accessible to a perturbative QCD treatment, one has to rely on QCD inspired phenomenological interaction models, in particular on string models based on the Gribov–Regge theory, like VENUS, QGSJET and SIBYLL. Recent results of EAS experiments are scrutinised in terms of such models, used as generators in the Monte Carlo EAS simulation code CORSIKA.

PACS numbers: 94.40.Lx, 94.40.Pa

1. Introduction

Cosmic rays is a radiation from the outer space, a feature of our environment like the starlight. It has been discovered nearly ninety years ago in the famous balloon ascents of the Austrian physicist Viktor Hess [1]. Since that time this phenomenon of nature has gained a lot of interesting and far reaching aspects of astrophysical and particle physics nature.

I had a look into the literature, what have been the hot topics discussed around 1930, when our distinguished and celebrated colleague Kasimir Grotowski was still in the cradle. It was the time when the new tool of electronic

* Presented at the Kazimierz Grotowski 70th Birthday Symposium "Phases of Nuclear Matter", Kraków, Poland, January 27–28, 2000.

coincidence devices, introduced by Walter Bothe, found extensive applications (see Ref. [2]). In 1929 Bothe and Kohlhörster [3] did the crucial experiment proving the corpuscular nature of the penetrating cosmic ray component, the muons produced in the secondary radiation. Bernard Rossi, spending some summer months in Bothe's institute improved the coincidence circuit for triple coincidences and prepared the later discovery of the air showers by Pierre Auger [4].

There is now a general consensus that the bulk of primary cosmic rays are accelerated at discrete sites in our Galaxy and roam around for ten millions years before incidentally hitting the Earth. Since they are overwhelmingly charged particles (protons, helium, carbon, nitrogen up to iron ions), they are deflected by the interstellar magnetic fields and have lost all memory of their origin when they accidentally arrive. This circumstance implies that

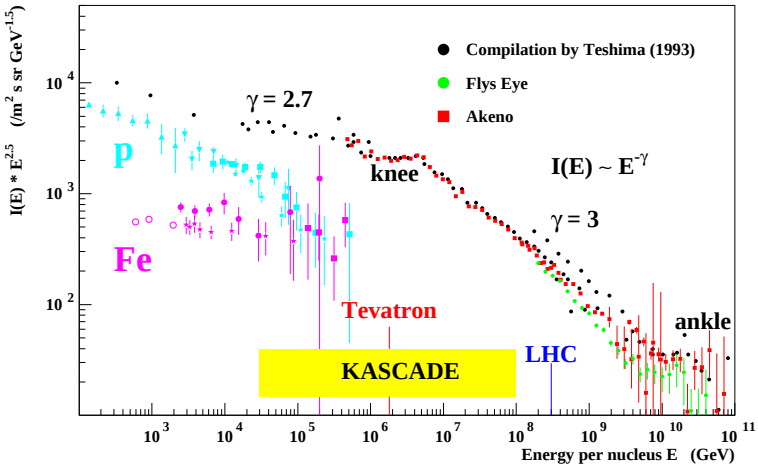

Fig. 1. Primary energy spectrum of cosmic rays (see Ref. [5])

their direction of incidence is no more related to the location of the sources. Hence the only observable quantities which may give us some information about their origin are the energy distribution and the elemental composition of the particle radiation. Their experimental determination are current topics of contemporary cosmic ray research, especially in energy regions which exceed the energies provided by artificial accelerators installed by man on our Earth.

The investigation of the detailed spectral shape and, in particular, of a conjectured variation of the mass composition in the region of the *so-called knee*, are the objectives of a number of current large scale experiments like the KASCADE experiment [6], set up in Karlsruhe (Germany).

The energy spectrum of primary cosmic rays comprises more than 12 orders of magnitude in the energy scale and extends to the enormous energy up to 10^{20} eV, the highest energies of individual particles in the Universe. The energy spectrum follows an overall power-law ($\propto E^{-2.7}$: Note that the flux is multiplied by $E^{2.7}$) with a characteristic distinct change around 10^{15} eV, called the "knee". The flux of primary cosmic rays falls from 1 particle/m^{2}s to 1 particle/km^{2}century at highest energies. A great deal of interest and current efforts concern the shape of the spectrum in the EeV-region, especially around 5×10^{19} eV, with the theoretically predicted Greisen–Zatsepin cut-off [7], due to the photo-interaction with the 2.7K-background radiation. The AGASA experiment in Akeno [8], in particular, has shown that this limit does not exist, and this fact is an issue of extreme astrophysical and cosmological relevance. The mystery of cosmic rays of highest energies has prompted the Pierre Auger Project [9].

In addition to the astrophysical aspects of *origin, acceleration and propagation* of the primary cosmic rays there is the historically well developed aspect of the interaction of high-energy particles with matter. Cosmic rays interacting with the atmosphere as target (on sea level it is equivalent to a lead bloc of 1m thickness) produce the full zoo of elementary particles and induce by cascade interactions intensive air showers (EAS), which we do observe with large extended detector arrays distributed in the landscapes, recording the features of different particle EAS components. The development of such air showers carries information about the hadronic interaction (though it has to be disentangled from the unknown nature and quality of the primary beam). When realising the present limits of man made accelerators, it is immediately obvious, why there appears a renaissance of interest in cosmic ray studies also from the point of view of particle physics. EAS observations of energies $> 10^{15}$ eV (Peta-electronvolt) represent an almost unique chance to test theoretical achievements of very high energy nuclear physics.

My lecture is directed to review some relevant aspects of hadronic interactions affecting the EAS development, illustrated with recent results of EAS investigations of the KASCADE experiment, especially of studies of the hadronic EAS component using the iron sampling calorimeter of the KASCADE central detector [10].

2. EAS development and hadronic interactions

Let us first recall what has to be specified for an understanding when a primary nucleus from the cosmos interacts with air nuclei of the high-altitude atmosphere. After an average of an interaction length, the nucleus is interacting, but typically only few nucleon participate. The spectator

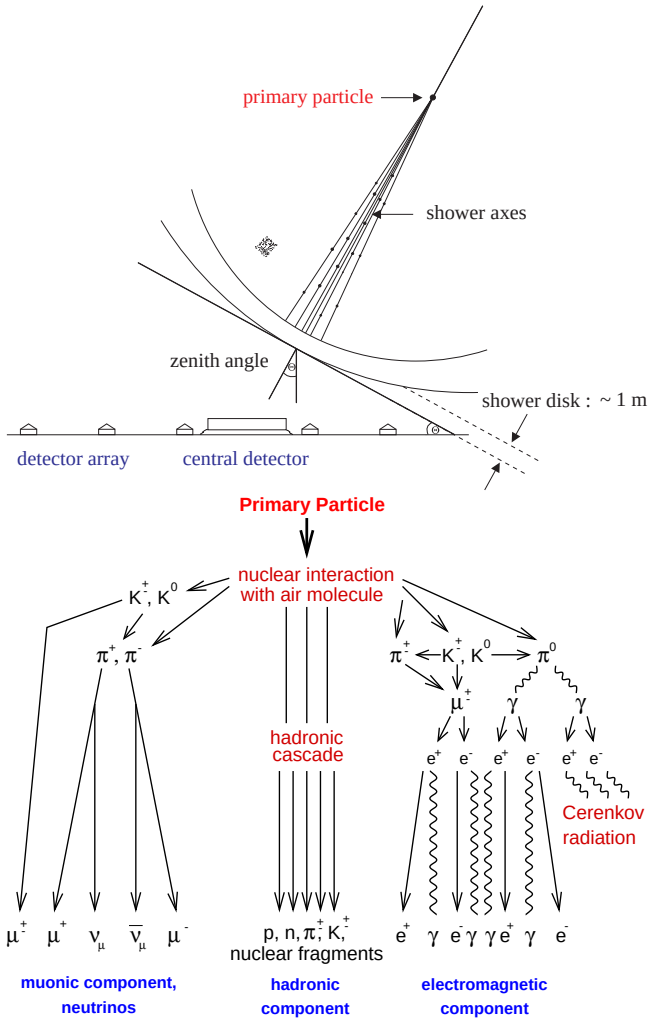

Fig. 2. Progeny of the EAS development

part breaks up in some fragments, which will in turn interact producing further spectator fragments. This process is iterated until finally all nucleons eventually interact.

Here the fragmentation pattern enters which may be described in detailed nuclear models, but mostly, in particular at high energies, it is common praxis to rely on a simple superposition model: a nucleus of mass number A and the total energy E_0 behaves after the first collisions like a swarm of A independent nucleons of the energy E_0/A.

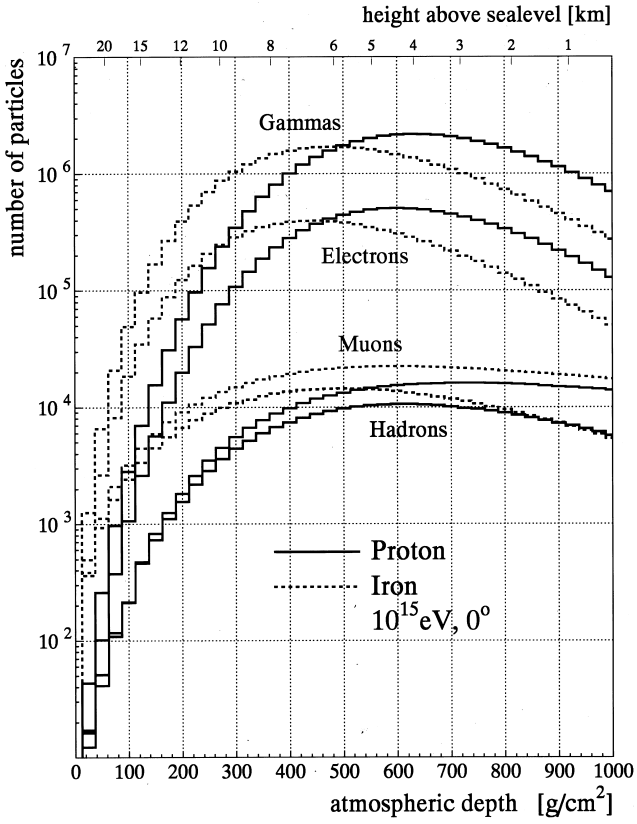

Fig. 3. The EAS longitudinal development from Monte Carlo simulations

Each nucleon interacting with the nuclei of the atmosphere produces many hadrons. Each hadronic particle *(i)* will go on interacting again or decaying, say after a travelling distance X with the probability:

$$P_i(X) = 1 - \exp\left\{-X\left(\frac{1}{\lambda_i} + \frac{1}{c\rho(h)\tau_i\gamma_i}\right)\right\} \tag{1}$$

λ_i= *mean free path length;* τ_i= *mean life time;* γ_i= *Lorentz factor;* $c\rho(h)$= *geometric path length.*

At very high energy the typical interaction length of a nucleon is $\lambda_N = 80\,\mathrm{g/cm^2}$, while a heavy nucleus can interact after only few $\mathrm{g/cm^2}$. We have then the evolution of hadronic cascades, which develops completely to an extensive air shower after ca. 12 interaction lengths for protons. At each step in the shower process the number of particles will grow while the

average energy will decrease. Thus the number of particles and the energy transferred to secondaries will reach a maximum at some atmospheric depth, which depends from the *energy*, from the *nature* from the primary particle and the details of the *interactions*.

Most of the produced particles in the hadronic interactions are pions and kaons, which can decay into *muons and neutrinos* before interacting, thus producing the most penetrating component of atmospheric showers. The most intensive component — *electrons and photons* — originates from the fast decay of neutral pions into photons, which initiate electromagnetic showers, thus distributing the originally high energy to millions of charged particles. The backbone of an air shower is the *hadronic component* of nucleons, pions and more exotic particles.

Figure 3 shows the longitudinal development of the total intensities of various EAS components: the sizes of the electromagnetic (N_e), the muon (N_μ) and the hadron (N_h) components, for the cases of 10^{15} eV proton and iron induced showers. Both cases differ by the atmospheric depth of the EAS maximum of the cascade.

The basic ingredients for the understanding of EAS are the *total cross sections* of hadron air collisions and the *differential cross sections for multiparticle production*. Actually our interest in the total cross section is better specified by the *inelastic* part, since the elastic part does not drive the EAS development.

Usually with ignoring coherence effects, the nucleon–nucleon cross section is considered to be more fundamental than the nucleus–nucleus cross section, which is believed to be obtained in terms of the first. Due to the short range of hadron interactions the proton will interact with only some, the so-called wounded nucleons of the target. The number could be estimated on basis of geometrical consideration, in which size and shape of the colliding nuclei enter. All this is mathematically formulated in the Glauber multiple scattering formalism, ending up with nucleon-nucleus cross sections.

Looking for the cross features of the particle production, the experiments show that the bulk of it consists of hadrons emitted with limited transverse momenta ($\langle P_t \rangle \sim 0.3\,\mathrm{GeV}/c$) with respect to the direction of the incident nucleon. In these "soft" processes the momentum transfer is small. More rare, but existing, are hard scattering processes with large P_t-emission.

It is useful to remind that cosmic ray observations of particle phenomena are strongly weighted to sample the production in forward direction. The kinematic range of the rapidity distribution (N(y) vs. y) for the Fermilab proton collider with the energy of 1.8 TeV in the c.m. system) is equivalent to the laboratory case (the cosmic ray situation) of 1.7 PeV. The energy flow $N(y) \cdot E$ is peaking near the kinematics limit. That means, most of the energy is carried away longitudinally.

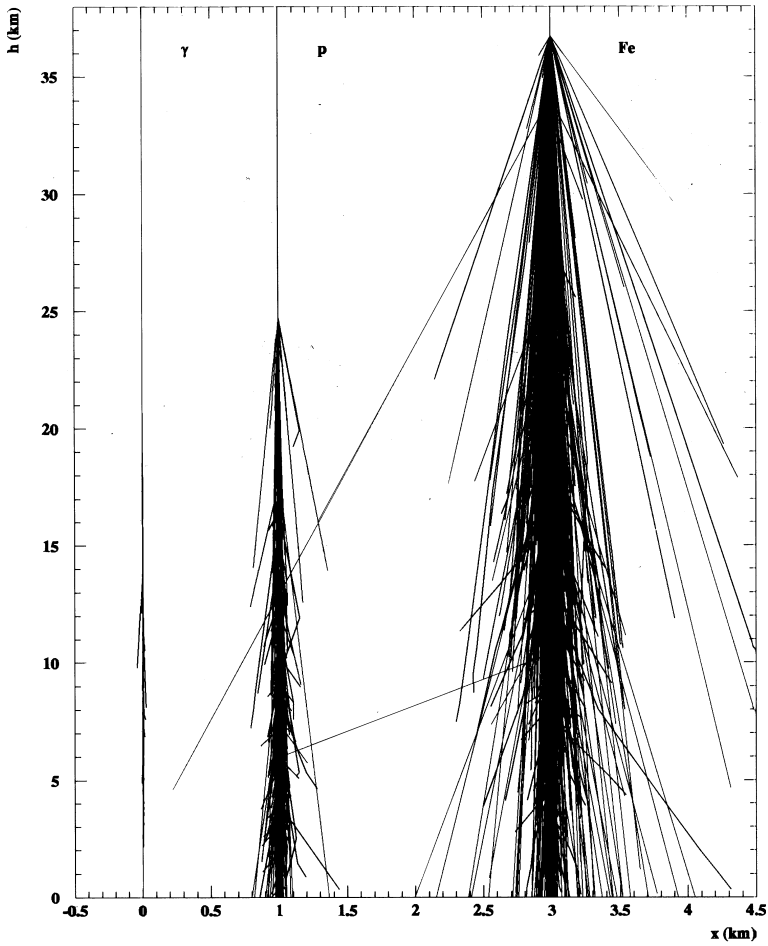

10^{15} eV EAS initiated
by a photon , by a proton and by a Fe nucleus

Energy threshold : 10 GeV

Since the photoproduction cross section of pions is some orders of magnitude smaller than the cross section for hadronic production, conventional EAS , initiated by UHE gamma rays are expected to be " muon poor ".

Fig. 4. Simulated EAS development

The graph displays simulated air-showers induced by a 10^{15} *eV photon, proton and Fe, respectively. Only particles with energies above 10 GeV are displayed. This cut reduces mainly the numerous electron and photons, whose energies are about 10 MeV in average on sea level (Note the scale). But one recognises the differences in the longitudinal development. The iron shower starts earlier and reaches the maximum earlier. At the same energy the intensity of the iron shower decreases faster after the maximum, since the primary energy is distributed to a larger number of interacting nucleons leading to lower-energy secondaries, being faster attenuated. That means that*

Fig. 5. Yeti-footprints

the intensity of the electron-gamma component arrives with smaller intensity at the observation level. On the other side the muon component of heavy ion

induced showers is more intensive due to the larger number of participants. The gamma shower shows much less fluctuations and is muon poor due to the small cross section of photoproduction muons.

The electromagnetic component is accompanied by an additional EAS phenomenon, the production of atmospheric Cerenkov light which carries further information about the shower development.

However, in ground-based experiments, in general, we are not in the situation to see the longitudinal development, we observe only the developed status of the air shower cascade at a certain observation level. From the observables there, that means from *the total intensities, the lateral and eventually the energy distributions of the different EAS components and their correlations*, we have to infer the properties of the primary particle, starting the cascade. The inherent fluctuations of the stochastic cascade processes are largely obscuring discriminating features.

Hence we are in the position like the Himalaya alpinists discovering puzzling large footprints as proof for the existence of the snowman Yeti (Fig. 5). Did not Kasimir Grotowski participate in that expedition in his younger days, collecting radioactive fall-out in high-mountain snow?

3. Hadronic interaction models as generators of Monte Carlo simulations

Microscopic hadronic interaction models, *i.e.* models based on parton–parton interactions are approaches, inspired by the QCD and considering the lowest order Feynman graphs involving the elementary constituents of hadrons (quarks and gluons). However, there are not yet exact ways to calculate the bulk of soft processes since for small momentum transfer the coupling constant α_s of the strong interaction is so large that perturbative QCD fails. Thus we have to rely on phenomenological models which incorporate concepts from scattering theory.

A class of successful models are based on the Gribov–Regge theory which finally leads to descriptions of colour exchange and re-arrangements of the quarks by string formation.

In the language of this theory the interaction is mediated by exchange particles so-called Reggeons. At high energies, when the non-resonant exchange is dominating, a special Reggeon without colour, charge and angular momentum, the Pomeron, gets importance. In a parton model the Pomeron can be identified as a complex gluon network or generalised ladders i.e. a colourless, flavourless multiple (two and more) gluon exchange. For inelastic interactions such a Pomeron cylinder of gluon and quark loops is cut, thus enabling colour exchange ("cut cylinder") and a re-arrangement of the quarks by a string formation.

We illustrate the model construction by discussing possible diagrams.

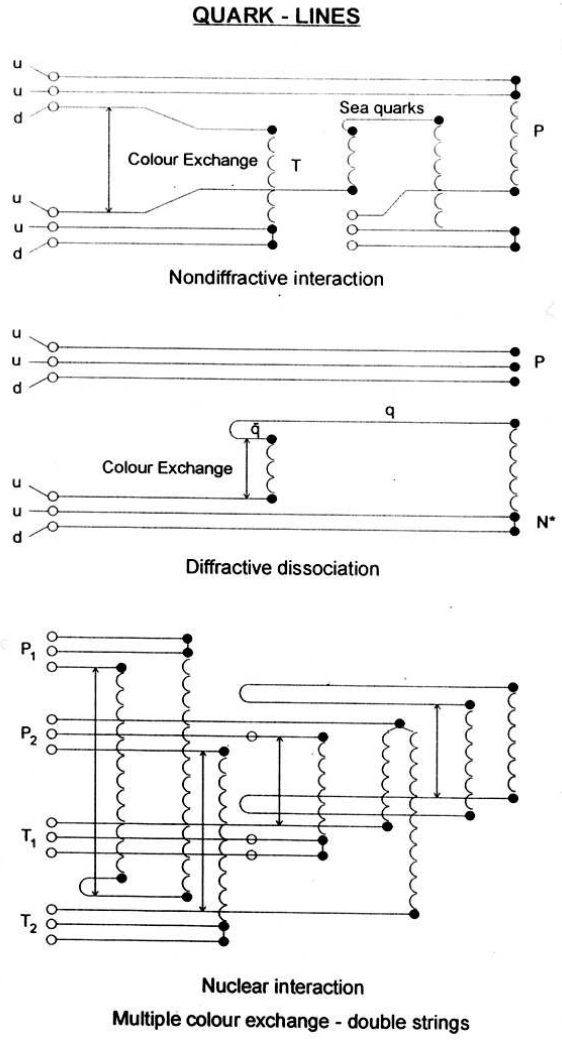

Fig. 6. Parton interaction diagrams

- *The interacting valence quarks of projectile and target rearrange by gluon exchange the colour structure of the system (the arrow indicates the colour exchange by opening the cylinder). As a consequence, constituents of the projectile and target (a fast quark and slow di-quark*

e.g.) for a colour singlet string with partons of large relative momenta. Due to the confinement the stretched chains start to fragment (i.e. a spontaneous $q\bar{q}$-production) in order to consume the energy within the string. We recognise a target string (T) and a projectile string (P), which are the only chains in pp collisions. In multiple collision processes in a nucleus, sea quarks are additionally excited and may mediate nucleon-A interactions. While in the intermediate step the projectile diquark remains inert, chains with the sea quark of the projectile are formed.

- *Most important are diffractive processes, signaled in the longitudinal momentum (x_F) distribution by the diffractive peak in forward directions. Here the interacting nucleon looks like a spectator, in some kind of polarisation being slowed down a little bit due to a soft excitation of another nucleon by a colour exchange with sea quarks (quark-antiquark pairs spontaneously created in the sea).*

- *There are a number of such quark lines, representing nondiffractive, diffractive and double diffractive processes, with single and multiple colour exchange.*

The various string models differ by the types of quark lines included. For a given diagram the strings are determined by Monte Carlo procedures. The momenta of the participating partons are generated along the structure functions. The models are also different in the technical procedures, how they incorporate hard processes, which can be calculated by perturbative QCD. With increasing energy hard and semihard parton collisions get important, in particular *minijets induced by gluon–gluon scattering.*

In summary, the string models VENUS [11], QGSJET [12], SIBYLL [13] and DPMJET [14], which we specifically use as generators in Monte Carlo simulations of air showers, are based on the Gribov–Regge theory and they describe soft particle interactions by exchange of one or multiple Pomerons. Inelastic reactions are simulated by cutting Pomerons, finally producing two colour strings per Pomeron which subsequently fragment into colour-neutral hadrons. The differences between the models are in some technical details in the treatment and fragmentation of strings. An important difference is that QGSJET and DPMJET are both able to treat hard processes, whereas VENUS, in the present form, does not. VENUS on the other hand allows for secondary interactions of strings which are close to each other in space and time.

These models are implemented in the Karlsruhe Monte Carlo simulation program CORSIKA [15] — now world-wide used — and to which we refer in the analyses of data.

4. The KASCADE apparatus

From the very beginning, when planning the KASCADE experiment [6] the set-up of a calorimeter for efficient studies of the hadronic component in the shower center has been foreseen with the intention of checking the predictions of hadronic interaction models.

The KASCADE detector array consists of an field array of 252 detector stations, arranged in a regular way in an area of $200 \times 200\,\mathrm{m}^2$, and of a complex central detector with a sampling calorimeter for hadron detection. The field detectors identify the EAS event, they provide the principal trigger

Fig. 7. The KASCADE experiment

(a coincidence in at least five stations), the basic characterisation (angle of incidence, shower axis and core location) and sample the lateral distribution of the electron–photon and muon component from which the shower size and quantities characterising the intensity and muon content of the showers are determined.

The central detector combines various types of detector installations with an iron sampling calorimeter of eight layers of active detectors.

The iron absorbers are 12–36 cm thick, increasingly in the deeper parts of calorimeter. Therefore the energy resolution does not scale as $1/\sqrt{E}$*, but is rather constant, slowly varying from* $\sigma/E = 20\%$ *at 100 GeV to* 10% *at 10 TeV. In total (including the concrete ceiling) the calorimeter thickness corresponds to 11 interaction lengths* ($\lambda_I = 16.7\,cm$ *Fe) for vertical muons. On top, a 5 cm lead layer absorbs the electromagnetic component to a sufficiently low level.*

The active detectors are 10,000 ionisation chambers using room temperature liquid tetramethylsilan (TMS) and tetramethylpentane (TMP) oper-

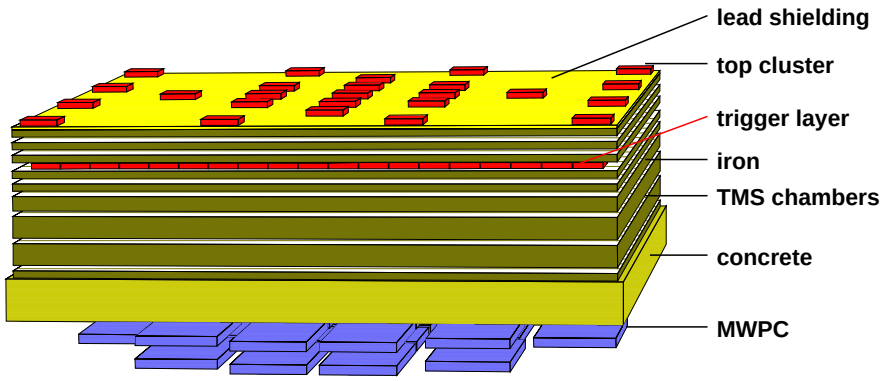

Fig. 8. Scheme of the KASCADE Central Detector

ated with a large dynamical range (5×10^4). This ensures that the calorimeter measures linearly the energy of single hadrons up to 25 TeV. The third layer of the calorimeter set-up is an "eye" of 456 plastic scintillators, which deliver a fast trigger signal. Independently from hadron calorimetry, it is used as additional muon detector and as timing facility for muon arrival time measurements. In the basement of the iron calorimeter there are position sensitive multiwire proportional chamber (MWPC) installed for specific studies of the structure of the shower core and of the EAS muon component with an energy threshold of about 2.4 GeV.

5. Test of EAS observables

The general scheme of the analysis of EAS observations is displayed in the diagram (Fig. 9). Using Monte Carlo simulations pseudo experimental data are constructed which can be compared with the real data. The king-way of the comparison is the application of advanced statistical techniques of multivariate analyses of nonparametric distributions [16,17]. These techniques consider also the influence of the fluctuations of the interaction processes.

The mass composition of cosmic rays in the energy region above 0.5 PeV is poorly known. Hence the comparison of simulation results based on different interaction models has to consider two extreme cases of the primary mass: *protons and iron nuclei*, and the criterion of our judgement of a model is directed to the question, if the data are compatible in the limits of the predicted extremes of protons and iron.

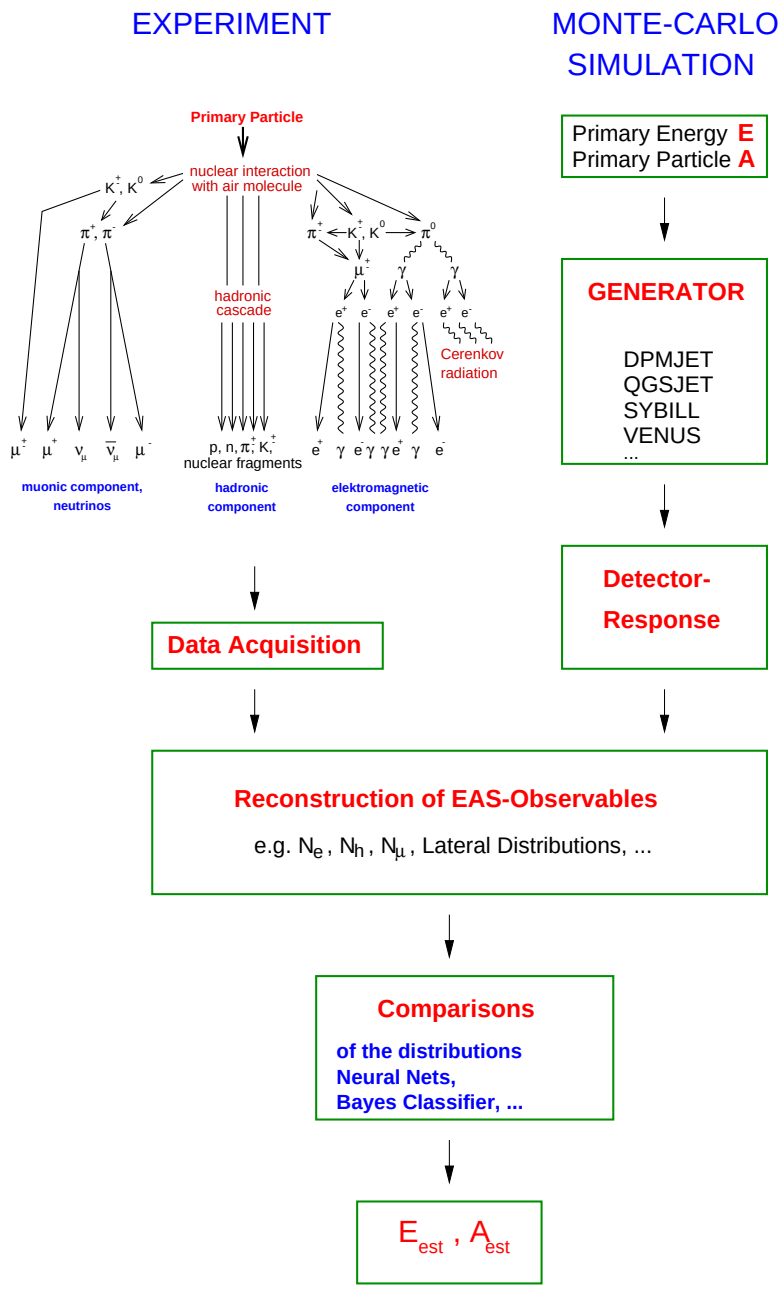

Fig. 9. General scheme of the analysis of EAS observations

In general we consider various shower observables like the number of hadrons in the shower core, their energy and spatial distributions in dependence from the shower sizes, characterising the registered EAS, in particular indicating the primary energy. Such parameters are:

- The shower size N_e, *i.e.* the total electron number.
- The muon content $N_\mu^{\rm tr}$ which the number of muons obtained from an integration of the lateral distribution in the radial range from 40 to 200 m. It has been shown that this quantity is approximately a mass independent energy estimator for the KASCADE layout, conveniently used for a first energy classification of the showers.

As an example of a test quantity we consider the *distribution of the energy fractions* of the shower hadrons. We display the energy fraction with respect to the most energetic hadron. For protons as primaries the leading particle is expected to produce one single particularly energetic "leading particle" accompanied by a broad distribution of lower energies. For iron primaries a more equal distribution is expected. The Monte Carlo simulations, here shown on the basis of the QGSJET model, confirm qualitatively this expectation. The physically meaningful region is the region between the two extremes, where the data should be found.

The upper side is the case for a lower primary energy of 2 PeV (identified with the muon number N'_μ — the truncated muon number $N_\mu^{\rm tr}$, as we say). There the data corroborate the model. For a higher primary energy of 12 PeV (at bottom), however, the simulations cannot explain the data, neither from proton nor iron nuclei induced showers.

Tentatively we may understand that in the simulations $E_{\rm max}$, the energy of the leading hadrons is too large. Lowering $E_{\rm max}$ would lead to a redistribution of the $E/E_{\rm max}$ distribution shifting the simulation curves in direction of the data. A further test quantity is related to the spatial granularity of hadronic core of the EAS. The graph shows the spatial distribution of hadrons (seen in a top view on the calorimeter) for a shower induced by a 15 PeV proton. The sizes of the points represent the energy (with a logarithmic scale). For a characterisation of the pattern a *minimum spanning tree* is constructed. All hadron points are connected by lines and the distances are weighted by the inverse sum of energies. The minimum spanning tree minimises the total sum of all weighted distances. The test quantity is the frequency distribution of the weighted distances.

Results are shown for two different bins of the truncated muon size or of the primary energy (2 and 12 PeV), respectively. Again we are lead to the impression that either the distribution pattern is not reproduced or the high energy hadrons are missing in the model.

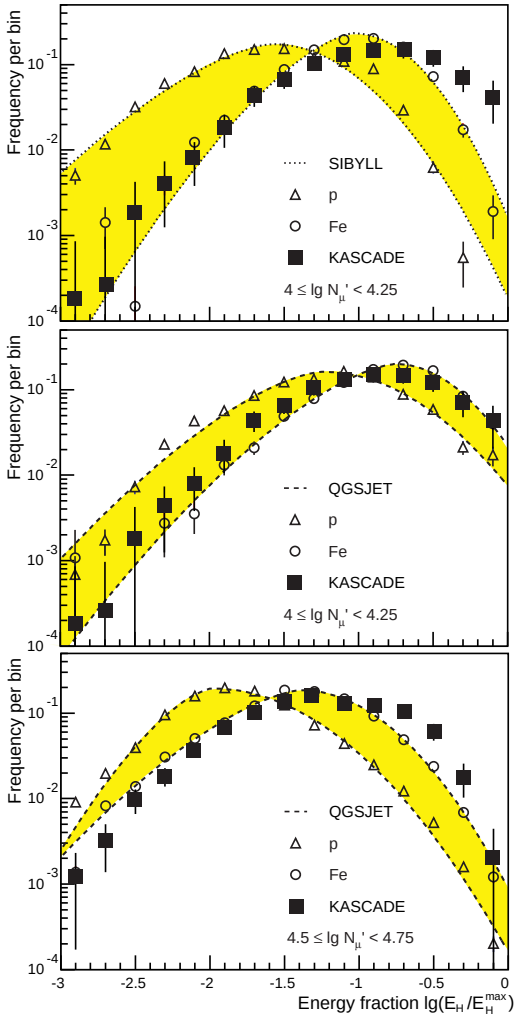

Fig. 10. The energy fraction of the EAS hadrons

Tentatively we may deduce from these indications, that the transfer of energy to the secondary — that what we phenomenologically call the *inelasticity* of the collision — is underestimated.

Such type of tests can be made with a number of shower observables, experimentally studied with the KASCADE apparatus, and for all the models under discussion. The interested audience may find the results in detail in a recent paper of the KASCADE collaboration [18].

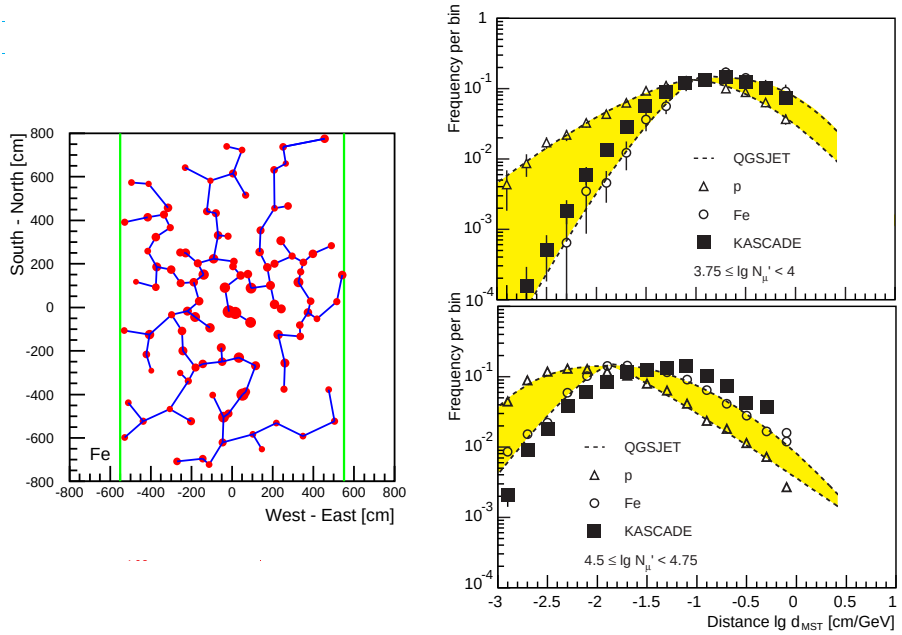

Fig. 11. Left: Minimum spanning tree. Right: Frequency distributions in the minimum spanning tree

6. Emulsion chamber experiments

The feature that the most energetic particles are concentrated in the core of the extensive air showers in their initial stages is the basis of the traditional emulsion chamber experiments on high altitudes, on Mt. Chacaltaya or Pamir *e.g.*, which collect with a special technique continuously strong interaction data and registrate also peculiar events, like Centauros.

A typical emulsion chamber device (Fig. 13) consists of two lead-X-ray film sandwich chambers (Gamma block and hadron block) of several squaremeters area, separated by a layer of carbon and some spacer. The radiation length in lead is very short (6.37 g/cm) compared to the nuclear interaction length (ca. 150 g/cm). Hence "atmospheric" photons and electrons initiate cascades very soon after entering the Gamma block, which contains some emulsion layers for identification. Hadrons on the other hand interact deeper in the upper chamber, in the carbon layer or in the lower chamber (if at all). Interactions of hadrons above the detector are expected to produce both hadrons and photons. A pure electromagnetic cascade in the atmosphere would manifest itself at the chamber as a group of cascades ("families") all starting near the top of the upper chamber. The Pamir chamber experiment

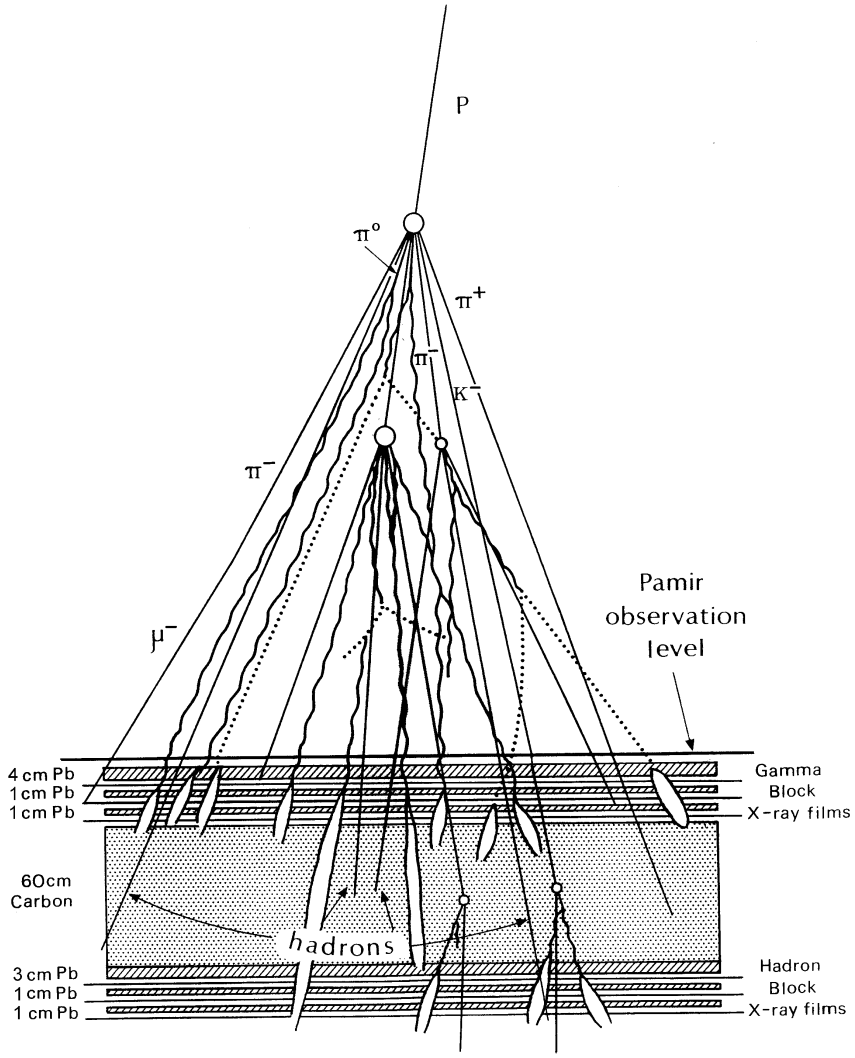

Fig. 12. Schematic structure of the Pamir chamber [19]

on 4370 m a.s.l. is able measure the flux of the electromagnetic particles in the range of 4–100 TeV produced by interactions of the primaries in the upper atmosphere. The particle flux can be estimated by the optical density of the measured spots in the X-ray films.

Andreas Haungs and Janusz Kempa [20] did carefully analyse such distributions, by calibrating the density of the spots in terms of the particle energies on basis of detector response simulations. In this way distributions,

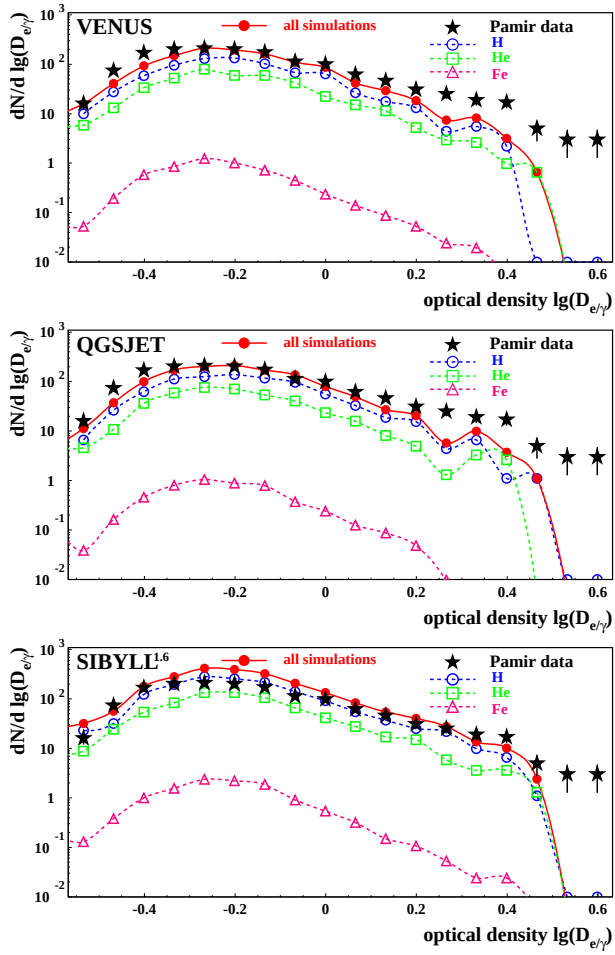

Fig. 13. Inclusive optical density spectrum observed in the working layer of the Pamir emulsion chamber compared with simulated spectra of different primaries for different interaction models [20]

observed in 11.5 sqm yr exposured film, could be compared with Monte Carlo simulations of primary particle interactions, assuming a mass spectrum from balloon-borne experiments in the energy range of 100–1000 TeV. Of course the observation is rather inclusive, averaged over the accepted energy range, the anticipated mass spectrum and the angle-of-incidence distribution. Figure 13 shows the results of the comparison with the model predictions.

The stars represent the data, *i.e.* the single particle spectrum measured with the working layer of PAMIR chamber. The other symbols represent the adequately normalised simulation results for different models as Monte Carlo generators. Differences between the VENUS and QGSJET models are found to be negligible, and ignoring some low energy effects, probably due to the scanning efficiency, there is good agreement, except at the highest energies. SIBYLL, however, in the current release and widely used for simulation studies, appears to be off. The predicted flux in forward direction proves to be too large.

7. Concluding remarks

From the investigation of a series EAS observables and comparisons with different hadronic interaction models, en vogue for ultrahigh energy collisions, we conclude with following messages:

- The model SIBYLL, in the present release, has problems, in particular when correlations with the muon content of the showers are involved. However it is fair to say, that the SIBYLL model experiences currently a thorough modification, just prompted by the KASCADE results.

- The model VENUS is in fair agreement with the data, but it indicates also some problems at high energies, when correlations with the shower sizes are considered.

- In the moment the model QGSJET, which includes the minijet production — in contrast to VENUS — reproduces sufficiently well the data, though it underestimates the number of high energy hadrons for high energies.

- In general there are tentative indications that the inelasticity (a phenomenological concept) in the fragmentation region is not well described, especially with increasing energy.

It should be noted that the experimentally defined concepts of "inelasticity" [19] and "leading particle", are not well identified in the theoretical models, since the secondary of the highest energy has often nearly no quark-structure overlap with the projectile-rest.

All current models are in a process of refinements and modifications. Actually somehow pushed by the experimental indications, there is a common enterprise of VENUS and QGSJET authors toward a model description: NeXus [21]. That is a unified approach combining coherently the Gribov–Regge theory and perturbative QCD. It should be realised: Faced with the experimental endeavour to set up giant arrays for astrophysical observations

at extremely high energies like the Pierre Auger experiment [9], the Monte Carlo simulations need certainly a safer ground of model generators. Hence in future our experimental efforts in KASCADE try to extend the array and to refine the present studies with results towards energies of the Large Hadron Collider.

I would like to express my thanks to Zbigniew Majka for organising this impressive symposium in honour of our distinguished colleague and friend Kasimir Grotowski, and for inviting me for this opportunity with a lecture dedicated to our celebrity. I feel privileged by a longstanding friendship with Kasimir Grotowski, with many fruitful scientific interactions and pleasant meetings. This lecture is based on experimental results of the KASCADE collaboration. I acknowledge various contributions and clarifying discussions of Dr. Andreas Haungs and Dr. Markus Roth.

REFERENCES

[1] V. Hess, *Z. Phys.* **12**, 998 (1911); *Z. Phys.* **13**, 1084 (1912).

[2] B. Rossi, *Nature* **125**, 636 (1930).

[3] W. Bothe, W. Kohlhörster, *Phys. Z.* **56**, 751 (1929).

[4] P. Auger *et al., Rev. Mod. Phys.* **11**, 288 (1939).

[5] J. Knapp, FZKA Report 5970, Forschungszentrum Karlsruhe 1997, p. 6.

[6] H.O. Klages *et al.* KASCADE collaboration, *Nucl. Phys.* (Proc. Suppl.) **52B**, 92 (1997).

[7] K. Greisen, *Phys. Rev. Lett.* **16**, 748 (1966); G.T. Zatsepin, V.A. Kuzmin, *JETP Lett.* **4**, 78 (1966).

[8] S. Yoshida *et al., Astroparticle Phys.* **3**, 105 (1995).

[9] J.W. Cronin, *Nucl. Phys.* (Proc.Suppl.) **28B**, 213 (1992).

[10] J. Engler *et al., Nucl. Instrum. Methods* **A427**, 528 (1999).

[11] K. Werner, *Phys. Rep.* **232**, 87 (1993).

[12] N.N. Kalmykov, S.S. Ostapchenko, A.I. Pavlov, *Nucl. Phys.* (Proc. Suppl.) **52B**, 17 (1997).

[13] R.S. Fletcher *et al., Phys. Rev.* **D50**, 5710 (1995).

[14] J. Ranft, *Phys. Rev.* **D51**, 64 (1995).

[15] J.N. Capdevielle *et al.*, KfK Report 4998, Kernforschungszentrum Karlsruhe (1992); D. Heck *et al.*, FZKA Report 6019, Forschungszentrum Karlsruhe (1998).

[16] A. Chilingarian, ANI — Nonparametric Statistical Analysis of High Energy Physics and Astrophysics Experiments, User's Guide, 1998.

[17] M. Roth, FZKA Report 6262, Forschungszentrum Karlsruhe.

[18] T. Antoni *et al.* KASCADE collaboration, *J. Phys. G: Nucl. Part. Phys.* **25**, 2161 (1999).

[19] C.R. Augusto *et al., Phys. Rev.* **D61**, 012003 (1999).

[20] A. Haungs, J. Kempa, J. Malinowski, Proc. 26th ICRC 1999 (Salt Lake City) HE 1.2.23.

[21] H. Drescher *et al., J. Phys. G: Nucl. Part. Phys.* **25**, 91 (1999).